

Introduction SSFP sequences consist of RF excitation pulses with flip angle α and phase angle ρ . If ρ is constant in successive excitations, the magnitude and phase profile is given by the dashed line in Fig.1. Changing the RF and acquisition phase by $\Delta\rho$ shifts the graphs. Adding multiple phase-cycled SSFP acquisitions in quadrature gives a relatively flat magnitude profile and, more importantly for PRF thermal mapping, leads to a fairly linear phase profile. If frequency shift maps linearly to a measurable phase shift in the combined image, it can be used for temperature estimation with the PRF shift.

Methods Computer simulations were performed to study the phase behavior (linearity and slope) for different imaging parameters (T_1 , T_2 , TR, flip) and number of phase cycles ($n=2$ with $\Delta\rho = 0^\circ, 180^\circ$; $n=3$ with $0^\circ, 120^\circ, 240^\circ$; $n=4$ with $0^\circ, 90^\circ, 180^\circ, 270^\circ$). In addition, the temperature dependent phase difference, $SNR_{\Delta\phi} = |\Delta\phi(\Delta T)|/\sigma_{\Delta\phi}$ with $\Delta\phi(\Delta T)$ being the phase change with temperature and $\sigma_{\Delta\phi}$ the uncertainty in the phase difference image, was determined and compared to a spoiled gradient echo sequence (SPGR). MR temperature maps of an agar phantom were acquired at 1.5T with the proposed balanced SSFP sequence (TR=10 ms, TE=TR/2=5 ms, flip=50°, $n=2-4$ phase cycles) and compared to SPGR images (TR/TE=30/15 ms). A temperature change was simulated by creating a linear field change of multiples of 0.64 Hz/cm with the gradient shim in x-direction. With a temperature induced PRF change at 1.5T of $\Delta f = 0.64$ Hz/°C, this corresponded to a maximum temperature change of 60°C at the edges of the phantom.

Results Results of the simulations are provided in Fig. 1 for $T_1/T_2=800/100$ ms, flip=40° and TE=TR/2=5 ms. For these values, increasing the averages to $n=4$ did not lead to any noticeable improvement in linearity, but would increase imaging time. Averaging $n=2$ images still showed a small amount of ripples in the phase profile. In general, the amount of ripple in both magnitude and phase decreases significantly as the flip angle increases or as the T_2/T_1 ratio decreases [1]. Depending on the tissue parameters more than three averages might be necessary, but in some cases as little as two averages could be sufficient. The slope of the phase change with frequency scales with TE. Shifting TE to later echo times in the TR window to increase the slope is possible, but was not investigated in this study.

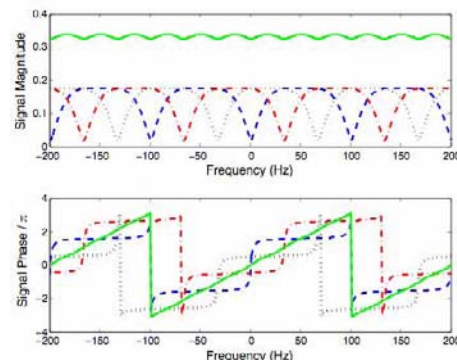


Figure 1: Magnitude and phase of the signal in balanced SSFP at TE = TR/2 for constant RF phase (dashed line), for $\Delta\rho = 120^\circ$ (dotted) and 240° (dash-dot). Combining the complex signals leads to the profile shown by the solid lines.

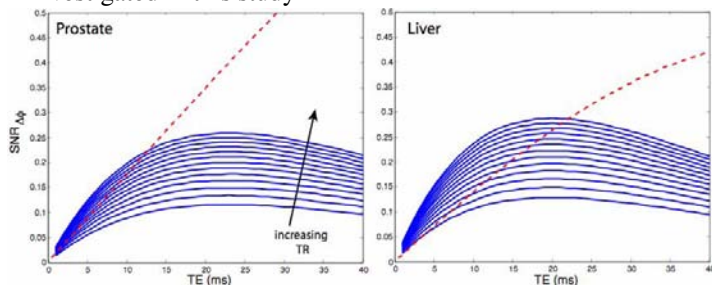


Figure 2: $SNR_{\Delta\phi}$ as a function of TE. The solid lines show curves for SPGR with TR=30-150 ms. The dashed line shows the curves for SSFP.

The SNR of the temperature dependent phase difference $SNR_{\Delta\phi}$ is plotted in Fig. 2 for values in prostate ($T_1/T_2=800/100$ ms) and liver ($T_1/T_2=490/40$ ms). The flip angle was optimized for maximum signal (SPGR $\alpha = \cos^{-1}(\exp(-TR/T_1))$; SSFP $\alpha = \cos^{-1}(T_1 - T_2)/(T_1 + T_2)$). The maximum $SNR_{\Delta\phi}$ in SPGR is reached at $TE=T_2^*$ and increases with increasing TR. The SSFP acquisition ($n=3$ averages) is shown for TE=TR/2. Although the curves include larger TE values, only values below approximately TR=15 ms (TE=7.5 ms) are practical. The graphs show that using the three-acquisition SSFP sequence can be advantageous when fast imaging of single slices or 3D imaging is desired. However, a general comparison is not possible, because the results are highly tissue and application dependent and the appropriate sequence has to be chosen on a case-by-case basis.

The MR imaging results are shown in Fig 3. The results show that the phase profile is linear enough to accurately measure the frequency change introduced by the gradient shim. For this phantom, combining only two phase cycles was sufficient to create the necessary linearity in the phase profile to measure the frequency change accurately.

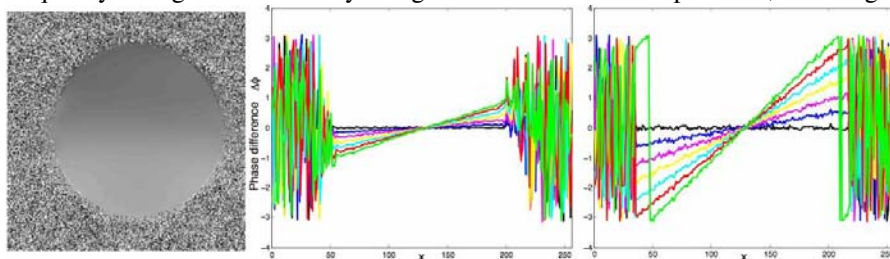


Figure 3: Phase difference image (left) from a three cycle combination showing the linear phase change in x-direction created by the gradient shim. The profile through the phantom is shown in the middle. The profile for SPGR is on the right.

Comparing the results to the SPGR acquisition shows that $\Delta\phi(\Delta T)$ is exactly three times larger in the SPGR images, as expected due to the three times longer TE compared to the SSFP acquisition, but the phase measurement is more noisy. Indeed, the temperature uncertainty σ_T in both methods was very similar; 1.1°C in SSFP and 1.0°C in SPGR.

Conclusions The results of simulations and phantom measurements have shown that combining the signals of multiple-acquisition phase-sensitive SSFP acquisitions results in a linear phase profile with frequency and can be used to measure temperature with the PRF shift method. Further studies are needed to evaluate if and in which tissues and applications the proposed method is better suited to monitor temperature than an SPGR sequence.

References [1] Bangertner N, Hargreaves B, Vasanawala S, Pauly J, Gold G, Nishimura D. Analysis of multiple-acquisition SSFP. Magn Reson Med 2004;51:1038-47.

Acknowledgements We would like to acknowledge our grant support, NIH ROI CA111891, NIH P41 RR009784, and NIH ROI CA077677.